

Simultaneously High Upconversion Efficiency and Large Anti-Stokes Shift by Using Os(II) Complex Dyad as Triplet Photosensitizer

Yaxiong Wei, Yuanming Li, Min Zheng, Xiaoguo Zhou,* Yang Zou, and Chuluo Yang*

To extend the triplet lifetime of photosensitizer, two new osmium complex dyads, with Os(phen)₃ as triplet energy donor and 9,10-diphenylanthracene (DPA) as energy acceptor, namely Os(phen)₃-DPA and Os(phen)₃-BDPA, are synthesized and characterized. The triplet lifetime of Os(phen)₃-DPA dyad is significantly extended to 1.1 μs by introducing triplet energy acceptor DPA to activate the intramolecular triplet energy transfer from the Os(phen)₃ to DPA units. By developing the triplet–triplet annihilation upconversion pairs of Os(phen)₃-DPA and 9-phenyl-10-(*p*-tolyl)anthracene, the deep-red light (at 663 nm) is upconverted to the blue-violet emission (at 415 nm) in 1,2-dichloroethane solution, and the highest upconversion quantum yield of 9.7% is achieved with a large anti-Stokes shift of 1.12 eV.

As one of the most important parameters of TTA upconversion system, the anti-Stokes shift is defined as the energy difference between the excitation photon and upconverted emission photon.^[13,14] A large anti-Stokes shift is very favorable for the application in photocatalytic water splitting, where the absorption is currently limited to ultraviolet light (<450 nm).^[10] However, as shown in Figure 1, the classic TTA upconversion process involves multistep downward energy transfer processes, in which the most energies are lost in intersystem crossing (ISC) and triplet–triplet energy transfer (TTET) processes,^[15–18] leading to that the reported

1. Introduction

Photon upconversion can produce high energy photons by means of low energy photons. Owing to low power density requirement and high upconversion quantum yield, triplet–triplet annihilation (TTA) upconversion is very promising in the various well known upconversion approaches.^[1–4] TTA upconversion has been applied in many fields, for example, the near-infrared to visible upconversion can increase the efficiency of single-junction photovoltaic cell to overcome the Shockley–Queisser limit;^[5–8] the visible to blue violet (or ultraviolet) upconversion can improve the efficiency of photocatalytic water splitting or organic reaction.^[9–12]

anti-Stokes shift is usually as small as less than 0.8 eV.^[19–22] A creative strategy to improve the anti-Stokes shift is to erase the energy loss of ISC by using the direct singlet-to-triplet (S-T) transition absorption molecule as photosensitizers, and minimizing the energy loss of TTET by selecting the appropriate acceptors.^[23–27]


In recent years, direct S₀→T₁ transition absorption of Os(II) complexes as triplet photosensitizers has been successfully applied in TTA upconversion.^[28–31] Kimizuka et al. demonstrated that a triplet photosensitizer, Os(btpy)₂²⁺, increased the anti-Stokes shift in TTA upconversion to 0.97 eV, but the upconversion quantum yield (Φ_{UC}) was only 2.7%.^[29] Recently, we have synthesized several new Os(II) complex photosensitizers, and a large anti-Stokes shift of 1.14 eV and Φ_{UC} of 5.9% has been reported in the Os-phen/DPA system.^[31] However, the triplet state lifetime of the Os(II) complex photosensitizer was as short as a few hundred nanoseconds, which apparently is a disadvantage for the TTET and upconversion. Thus, to further improve TTET efficiency and TTA upconversion quantum yield, a long triplet lifetime of direct S–T excitation photosensitizer is highly desirable. Very recently, Kimizuka et al. have designed a new direct S-T transition photosensitizer of Os(peptpy)₂²⁺, and its triplet lifetime has been prolonged to 23 μs, promoting Φ_{UC} to 5.9%.^[32]

In this work, aiming to extend the triplet lifetime of photosensitizer, we have designed and synthesized two new Os(phen)₃-DPA complex dyads (Figure 2a), with Os(phen)₃ as triplet energy donor (T₁ = 1.80 eV)^[31] and 9,10-diphenylanthracene (DPA) as energy acceptor (T₁ = 1.75 eV)^[33] to switch the short-lived ³MLCT state (³[Os(phen)₃] ≈ 10² ns) to the long-lived ³DPA* (≈1.1 μs). By sensitizing 9-phenyl-10-(*p*-tolyl)anthracene (DPA-Me) triplet with Os(phen)₃-DPA dyad, the deep-red light (at 663 nm) is upconverted to the blue–violet emission

Dr. Y. Wei, Dr. Y. Zou, Prof. C. Yang
Shenzhen Key Laboratory of Polymer Science and Technology
College of Materials Science and Engineering
Shenzhen University
Shenzhen 518060, China
E-mail: clyang@szu.edu.cn

Dr. Y. Wei
College of Physics and Optoelectronic Engineering
Shenzhen University
Shenzhen 518060, China

Dr. Y. Li, Dr. M. Zheng, Prof. X. Zhou
Department of Chemical Physics
University of Science and Technology of China
Hefei, Anhui 230026, China
E-mail: xzhou@ustc.edu.cn

 The ORCID identification number(s) for the author(s) of this article can be found under <https://doi.org/10.1002/adom.201902157>.

DOI: 10.1002/adom.201902157

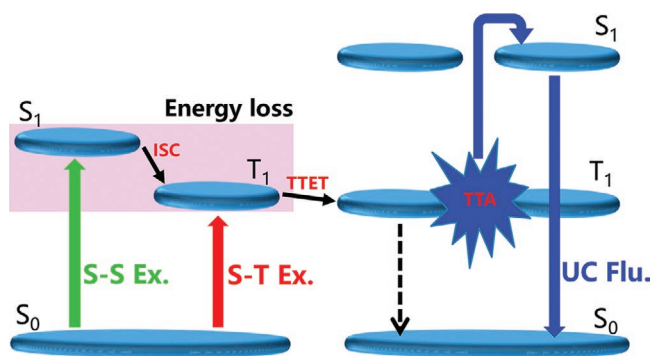


Figure 1. The Jablonski diagram of the representative TTA upconversion system.

(at 415 nm) in 1,2-dichloroethane solution, and the highest upconversion quantum yield of 9.7% and a large anti-Stokes shift of 1.12 eV is simultaneously achieved.

2. Results and Discussions

2.1. The Steady-State Spectra

The molecular structures of Os(phen)₃-DPA dyads were shown in Figure 2a, with DPA unit connected to Os(phen)₃ by single bond or phenyl to realize intramolecular triplet energy transfer (ITET). To achieve the highest Φ_{UC} and large anti-Stokes shift, two triplet acceptors with the feasible triplet energy, DPA and DPA-Me, were tested. Finally, DPA-Me (T₁ = 1.74 eV) was selected as triplet acceptor for TTA upconversion measurements due to its better performance. The new photosensitizers and acceptor were synthesized and fully characterized (Figures S1–S14, Supporting Information).

As shown in Figure 2b, the steady-state spectra of Os(II) complexes were measured in 1,2-dichloroethane solution. Os(phen)₃ displayed a direct S-T metal to ligand charge transfer (MLCT) absorption band at 660 nm (ε = 3500 cm⁻¹ M⁻¹) with tails extending over 705 nm, and two intense singlet–singlet absorption peaks at 432 and 481 nm. With excitation of the S-T MLCT band at 663 nm, the phosphorescence emission from its

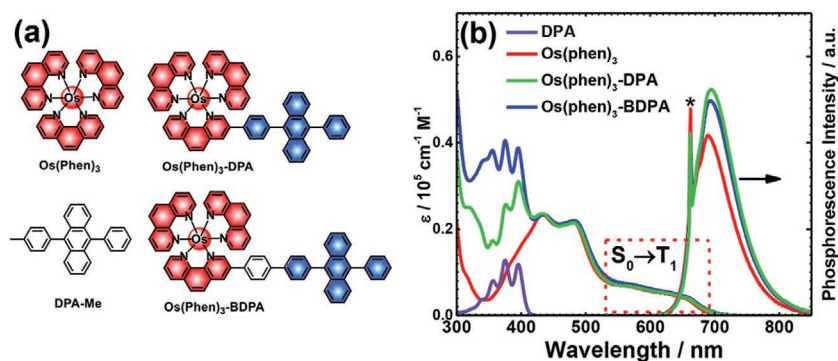


Figure 2. a) The molecular structure of photosensitizers and acceptor (DPA-Me). b) The steady-state absorption and phosphorescence emission (λ_{ex} = 663 nm) spectra of Os(phen)₃, Os(phen)₃-BDPA, Os(phen)₃-DPA, and DPA. c = 1 × 10⁻⁵ M, 1,2-dichloroethane as solvent.

triplet state was observed with a peak at 690 nm (Figure 2b). Such small Stokes shift of 0.07 eV implies small energy loss of ISC process. For Os(phen)₃-DPA and Os(phen)₃-BDPA, similar MLCT absorption bands at ≈660 nm were also observed, assigning to the contribution of Os(phen)₃ unit. Meanwhile, a few new absorption bands appeared at 300–400 nm that can be attributed to the energy acceptor DPA unit. The absorption spectrum of Os(phen)₃-DPA dyads does not equal the simple sum of Os(phen)₃ and DPA units, indicating that the electronic interaction between energy donor and acceptor units in ground state is weak but non-negligible.^[34] Moreover, the phosphorescence emission of Os(phen)₃-DPA and Os(phen)₃-BDPA were observed at 693 and 694 nm, respectively, (Figure 2b) which were very close to that of Os(phen)₃, indicative of their close triplet energies. The phosphorescence quantum yields (Φ) of the three photosensitizers were determined to be 5.5% for Os(phen)₃, 7.0% for Os(phen)₃-DPA, and 6.6% for Os(phen)₃-BDPA. Compared with Os(phen)₃, the quantum yields of Os(phen)₃-DPA and Os(phen)₃-BDPA were slightly enhanced. Table 1 summarized these photophysical data.

2.2. Nanosecond Transient Absorption Spectra

Figure 3a–c displayed the nanosecond transient absorption spectra of the Os(II) complexes with photoexcitation at 532 nm. Os(phen)₃ (Figure 3a) exhibited two negative absorption bands at 487 nm (ground state bleaching) and 705 nm (phosphorescence emission), and the lifetime of its triplet state was determined to be 0.36 μs from the decay rates of phosphorescence emissions (Figure 3d). Compared to Os(phen)₃, similar results were observed for Os(phen)₃-DPA (Figure 3b), but a new positive absorption peak appeared at 450 nm that is the characteristic absorption peak of ³DPA*. Hence, the triplet energy transfer from Os(phen)₃ to DPA units definitely occurred when Os(phen)₃-DPA was excited at 532 nm. Our theoretical calculations on triplet spin density surfaces also proved that the lowest triplet state of Os(phen)₃-DPA dyad is located at the DPA unit (Figure 4b).

For Os(phen)₃-DPA, the triplet state lifetime of DPA unit was determined to be 1.3 μs by using the single-exponential fitting of the decay curve at 450 nm (Figure S15, Supporting Information). Although the similar phosphorescence emission was observed for Os(phen)₃ and Os(phen)₃-DPA (Figure 2b), their phosphorescence lifetimes is drastically different, for example, the double exponential decay was obtained for Os(phen)₃-DPA with the characteristic lifetimes of 0.33 μs (55%) and 1.1 μs (45%). Apparently, the short-lived component is attributed to the decay of ³Os(phen)₃* itself, while the long-lived component is very close to the lifetime of ³DPA* (1.3 μs), indicating that the phosphorescence decay of Os(phen)₃-DPA occurs along two competing pathways. The most feasible pathway is the thermally reverse triplet energy transfer (RTET) from DPA to Os(phen)₃ units (Figure 4a) due to their near degenerate energies. Although the ³MLCT state of Os(phen)₃ unit (1.79 eV)

Table 1. The photophysical data of three photosensitizers.

Compound	λ_{Abs} [nm]	λ_{Em} [nm] ^{a)}	Triplet energy [eV]		τ [μs] ^{d)}	Φ^{e}
			Theory ^{b)}	Experiment ^{c)}		
Os(phen) ₃	432/481	690	–	1.80	0.36	0.055
Os(phen) ₃ -DPA	356/376/395/435/482	693	1.74	1.79	0.33(55%)/1.1(45%)	0.070
Os(phen) ₃ -BDPA	355/375/395/435/482	694	1.72	1.79	0.24(32%)/1.2(68%)	0.066

^{a)}The peak wavelength of phosphorescence emission ($\lambda_{\text{ex}} = 663$ nm); ^{b)}The DFT calculated values; ^{c)}Calculated with the phosphorescence emission peak; ^{d)}The values in parentheses are the fitted weights of the corresponding delay pathways; ^{e)}Phosphorescence quantum yield, using methylene blue as a standard ($\Phi_{\text{FL}} = 3\%$).

is slightly higher than the triplet energy of DPA unit (1.74 eV), such small difference can be readily overcome by the thermal activated energy at room temperature. Thus, the thermal RTET from DPA to Os(phen)₃ units could occur. Similar results were also observed for Os(phen)₃-BDPA (Figure 3c,f), with the characteristic absorption peak of ³DPA* at 450 nm and the triplet state lifetime of 0.24 μs (32%) and 1.2 μs (68%).

2.3. TTA Upconversion Spectra

Interestingly, under photoexcitation at 663 nm (1.87 eV), the Os(phen)₃-DPA/DPA-Me mixed solution showed a significantly upconverted blue–violet emission at 415 nm (2.99 eV) (Figure 5a). The anti-Stokes shift was 1.12 eV, which is comparable to the largest values (1.14 eV) reported in literatures.^[31] As shown in Figure 5b, Φ_{UC} with the concentration of DPA-Me were investigated. For three photosensitizers, Φ_{UC} was increased rapidly in

low concentration of DPA-Me (<10 mM), and became saturated. With the DPA-Me concentration of 10 mM, the maximal Φ_{UC} values of Os(phen)₃-DPA, Os(phen)₃-BDPA, and Os(phen)₃ were determined to be 9.7%, 5.3%, and 5.6%, respectively, the former of which was nearly twice as much as that of Os(phen)₃/DPA (5.9%, anti-Stokes shift of 1.14 eV).^[31] Such a significant improvement of TTA upconversion quantum yield is attributed to the prolonged triplet state lifetimes of the new Os(II) dyads by ITET and RTET. In addition, as discussed in the dynamic fitting with Stern–Volmer equation (Figures S16 and S17, Supporting Information), with the prolonged lifetime of photosensitizer, the bimolecular quenching rate constants k_{q} of triplet dyads by DPA-Me were significantly increased from $1.33 \times 10^9 \text{ M}^{-1} \text{ s}^{-1}$ in Os(phen)₃ to $2.55 \times 10^9 \text{ M}^{-1} \text{ s}^{-1}$ in Os(phen)₃-DPA, and $2.21 \times 10^9 \text{ M}^{-1} \text{ s}^{-1}$ in Os(phen)₃-BDPA.

Moreover, as suggested by Zhao et al.,^[1] the light-harvesting ability of photosensitizer should also be taken into account to assess the entire upconversion system. According to an overall

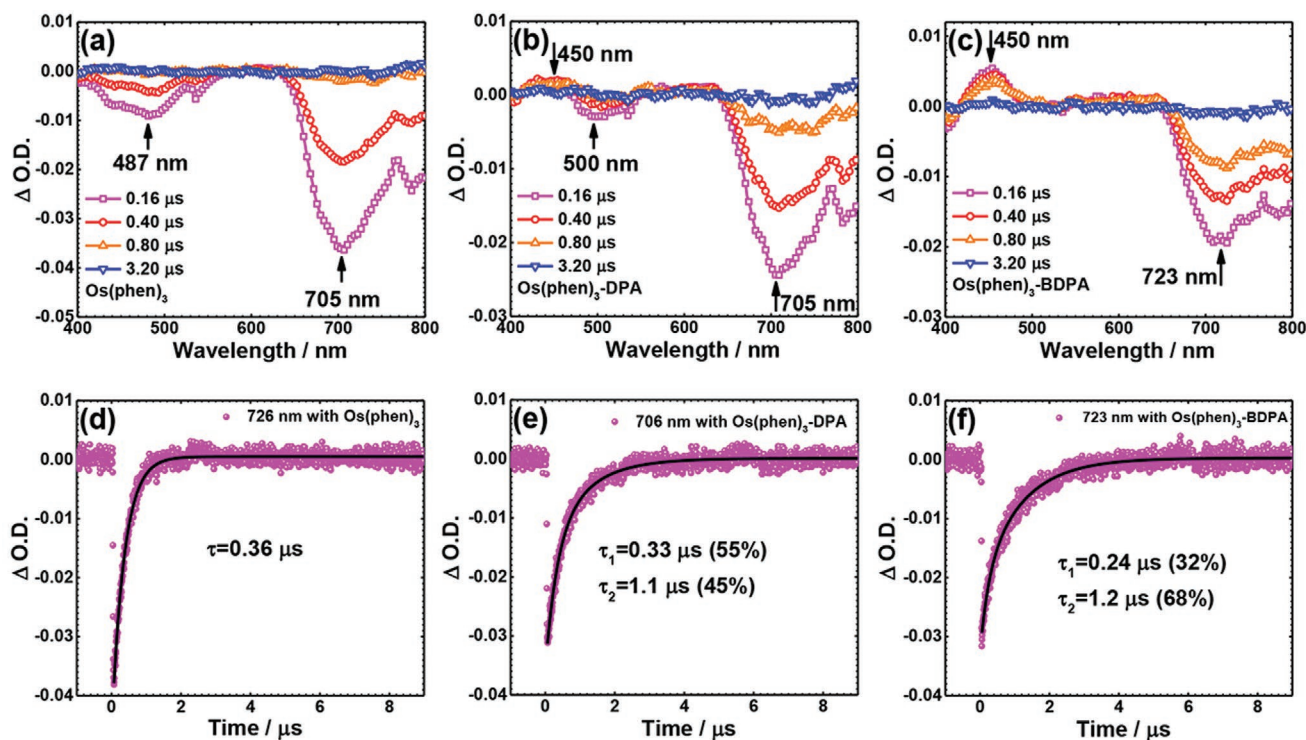


Figure 3. a–c) The nanosecond transient absorption spectra and d–f) decay kinetic curves of Os(phen)₃, Os(phen)₃-DPA, Os(phen)₃-BDPA, respectively. $c(\text{photosensitizer}) = 1 \times 10^{-5} \text{ M}$, 1,2-dichloroethane as solvent, $\lambda_{\text{ex}} = 532$ nm.

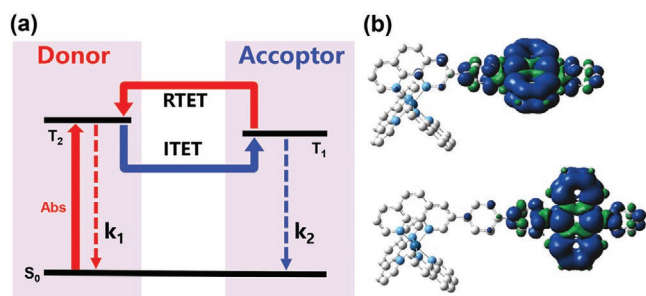


Figure 4. a) The Jablonski diagram of the intramolecular triplet energy transfer (ITET) and thermally reverse triplet energy transfer (RTET). b) Spin density surfaces of the triplet states of Os(phen)₃-DPA and Os(phen)₃-BDPA. The calculations were performed at the B3LYP/6-31G(d) level.

upconversion capability, $\eta = \varepsilon \times \Phi_{UC}$ (ε is the molar extinction coefficient), the η value for Os(phen)₃-DPA/DPA-Me is 315 M⁻¹ cm⁻¹, which is much larger than the previously reported value (94 M⁻¹ cm⁻¹).^[32]

It is well known that the upconverted fluorescence intensity shows a quadratic dependence on excitation power at low intensities and a linear dependence at high power densities.^[35,36] Thus, an important parameter, I_{th} , is defined as the threshold excitation power density of TTA upconversion. The upconversion emission intensity was plotted as a function of excitation light power density at different concentration of DPA-Me (Figure 5c). The Os(phen)₃-DPA/DPA-Me system showed a slope change from

2 to 1 in the double logarithmic plot with the increase of laser power density. The I_{th} value was determined to be 960 mW cm⁻² for Os(phen)₃-DPA with the DPA-Me concentration of 0.4 mM, and reduced to 132 mW cm⁻² in a higher DPA-Me concentration of 10 mM. This relationship agrees well with the fact that the TTET efficiency can be enhanced with the increase of acceptor concentration. Notably, the observed I_{th} values of 132 mW cm⁻² is lower than that of the previous Os(phen)₃/DPA system (200 mW cm⁻²) under the identical conditions.^[31] Thus, in the Os(phen)₃-DPA/DPA-Me system, the extended triplet state lifetime of photosensitizer significantly improves the TTET and TTA efficiencies, rendering the reduction I_{th} value.

To our surprise, Os(phen)₃-DPA and Os(phen)₃-BDPA with similar structures and triplet lifetimes showed different upconversion quantum yields. To understand in-depth the microscopic mechanisms, the triplet energies of Os(II) complexes and acceptor were measured and calculated (Figure 5d). The triplet energies of Os(phen)₃ and DPA unit in Os(phen)₃-DPA is 1.79 and 1.74 eV, respectively, both of which are higher than or equal to that of the DPA-Me acceptor (1.74 eV). Thus, the intermolecular TTET can efficiently occur between the day and DPA-Me, promoting the formation of triplet DPA-Me and then the TTA upconversion. In Os(phen)₃-BDPA, the triplet energy of Os(phen)₃ unit is 1.79 eV and high enough for the intermolecular TTET. However, owing to conjugative effect, the triplet energy of BDPA unit was reduced to 1.72 eV, which was slightly lower than the triplet DPA-Me (1.74 eV). As a result, the

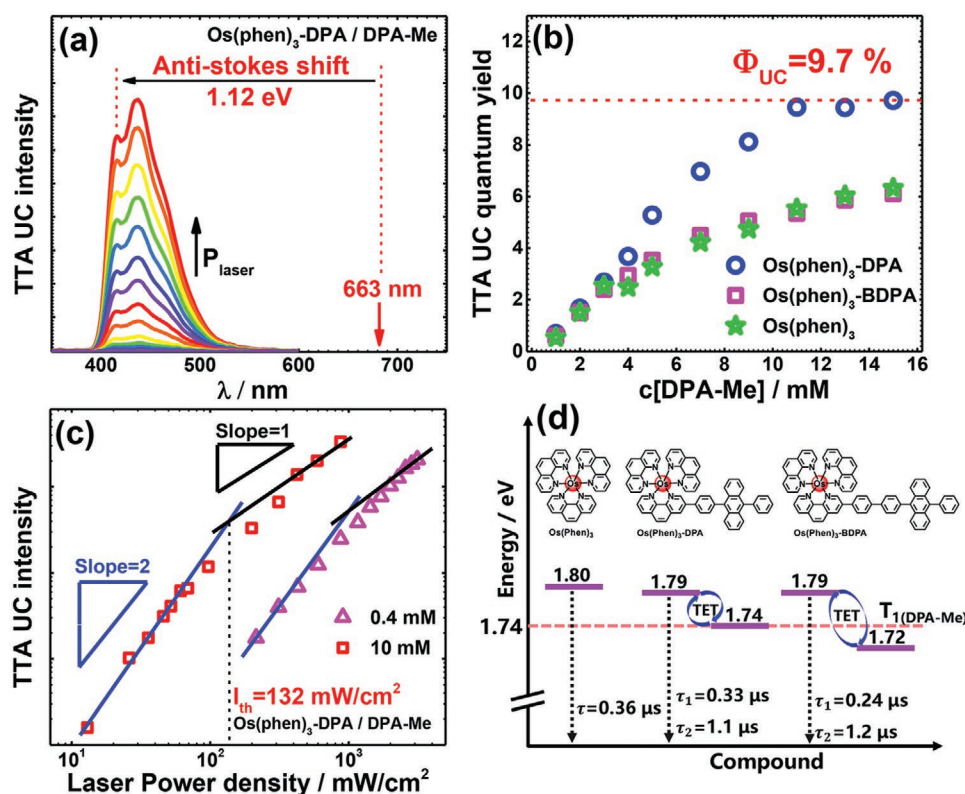


Figure 5. a) Upconverted fluorescence emission spectra under different excitation power densities with Os(phen)₃-DPA/DPA-Me system, $c(\text{DPA-Me}) = 0.4$ mM. b) Dependence of the overall TTA upconversion quantum yield on DPA-Me concentration. c) Double logarithmic plot of the upconverted fluorescence intensity as a function of excitation power density in Os(phen)₃-DPA/DPA-Me system, $c(\text{DPA-Me}) = 0.4$ and 10 mM. d) Triplet energy of Os(II) complexes and acceptor. 1,2-dichloroethane as the solvent, $c(\text{photosensitizer}) = 1 \times 10^{-5}$ M, $\lambda_{ex} = 663$ nm.

TTET efficiency between Os(phen)₃-BDPA and DPA-Me was relatively low. These results indicate that the efficiency of TTET and TTA upconversion can be enhanced by suitably matching the triplet energy levels of photosensitizer and acceptor.

3. Conclusion

In conclusion, we developed two new Os(II) complex dyads for high TTA upconversion efficiency and large anti-Stokes shift. The direct S-T transition of Os(II) complex removed the energy loss in ISC process, minimized the energy loss of TTET by selecting the appropriate acceptor (DPA-Me), and as a result, a large anti-Stokes shift in TTA upconversion of 1.12 eV was achieved. Moreover, based on the efficient ITET from the Os(phen)₃ to DPA units in Os(phen)₃-DPA, the triplet lifetime was extended to 1.1 μs and the upconversion quantum yield was thus boosted to 9.7%, which is nearly twice as much as that of Os(phen)₃. This work provides a design guidance for photosensitizer with both high upconversion efficiency and large anti-Stokes shift for TTA upconversion, which will significantly promote TTA upconversion applications in photocatalytic water splitting and biological imaging. The further application in the related fields, for example, TTA upconversion in solid or film devices, is undergoing.

4. Experimental Section

Commercial Instruments: High-resolution TOF mass spectra were performed on SCIEX TripleTOF6600 nanoLCMS. Mass spectra were recorded with 5800 MALDI-TOF/TOF (AB SCIEX). ¹H NMR spectra were measured with a 500 MHz spectrophotometer (Avance III 500, Bruker), where DMSO-d₆ or CDCl₃ were used as solvents and tetramethylsilane (TMS) was the standard for which δ = 0.00 ppm. Steady-state UV-vis absorption spectra were recorded with a spectrophotometer (UV-2600, Shimadzu).

Nanosecond Time-Resolved Transient Absorption Spectra: Nanosecond time-resolved transient absorption spectra were measured with a home-built laser flash photolysis system. The second harmonic 532 nm of a Q-switched Nd:YAG laser (Dawa-100, Beamtech) was used as the pulsed excitation light (pulse duration 8 ns, repetition rate of 10 Hz, pulse energy <10 mJ per pulse). A 500 W xenon lamp was used as the analyzing light, and passed through a quartz cuvette (10 mm × 10 mm) perpendicularly with the pulsed laser. A monochromator equipped with a photomultiplier was used to record transient absorption spectra within a wavelength range of 300–800 nm. The typical spectral resolution was less than 1 nm. A kinetic curve of intermediate was averaged by multishots and recorded with an oscilloscope (TDS3052B, Tektronix). All the solutions were deoxygenated by purging with high purity argon (99.99%) for about 20 min prior to measurements.

TTA Upconversion Spectra: TTA upconversion spectra were recorded using a home-made fluorescence emission spectrometer. A semiconductor laser (663 nm) was selected as the excitation light source. The diameter of the laser spot in sample cell region was ≈3.5 mm. In the TTA upconversion experiments, the solutions mixing photosensitizer and acceptor were kept in a temperature-controlled quartz cuvette (10 mm × 3 mm), deoxygenated by purging with high-purity argon (99.99%) for at least 20 min, and the gas flow was kept during measurements. In experiments, the upconverted fluorescence of acceptors was collected and detected with a commercial fiber-optic spectrometer (ULS2048-2-USB2, AvaSpec), under photoexcitation at 663 nm. The spectral resolution was ≈0.5 nm.

Density Functional Theory Calculations: Geometries of the compounds were optimized using density functional theory (DFT) with the B3LYP function and 6–31G(d) basis set. No imaginary frequencies were confirmed for all the optimized structures. The spin density surfaces of the complexes, and the energy gaps between ground state and lowest triplet state were calculated with time-dependent DFT (TD-DFT) level using the same basis set. The vertical excitation energies were directly compared with absorption spectra, and the corresponding electronic transitions were identified subsequently. The PCM model was applied to evaluate the solvent effect. All these calculations were performed with the Gaussian 09W program package.^[37]

TTA Upconversion Quantum Yields: Using methylene blue as the standard, steady-state absorbance spectra of the sample and the standard in diluted solutions were recorded using a fluorescence spectrometer, where their absorbance at excitation wavelength was not more than 0.05. Through integrating the band area in emission spectra of the sample and the standard, the quantum yield of the sample could be determined. In the present experiments, the TTA upconversion quantum yields, Φ_{UC}, were calculated as Equation (1)

$$\Phi_{UC} = 2\Phi_{std} \times \left(\frac{A_{std}}{I_{std}} \right) \times \left(\frac{I_{sam}}{A_{sam}} \right) \times \left(\frac{\eta_{sam}}{\eta_{std}} \right)^2 \quad (1)$$

where A, I, and η are the absorbance intensity, the integrated emission intensity, and the refractive index of the solvents used for standard and samples. It was noted that a factor of 2 multiplied to Equation (1), in order to make the maximum quantum yield to be unity.

Supporting Information

Supporting Information is available from the Wiley Online Library or from the author.

Acknowledgements

The authors gratefully acknowledge financial support from the Shenzhen Science and Technology Program (KQTD20170330110107046), the Shenzhen Technology and Innovation Commission (JCYJ20180507182244027), and National Natural Science Foundation of China (Grant No. 51703131, 91833304, 21873089, and 21573210). They thank the Instrumental Analysis Center of Shenzhen University for analytical support.

Conflict of Interest

The authors declare no conflict of interest.

Keywords

anti-Stokes shift, direct singlet–triplet transition, osmium(II) complexes, photosensitizers, triplet–triplet annihilation upconversion

Received: December 26, 2019

Revised: February 5, 2020

Published online: February 28, 2020

[1] J. Zhao, S. Ji, H. Guo, *RSC Adv.* **2011**, *1*, 937.

[2] C. Ye, L. Zhou, X. Wang, Z. Liang, *Phys. Chem. Chem. Phys.* **2016**, *18*, 10818.

- [3] A. B. Pun, L. M. Campos, D. N. Congreve, *J. Am. Chem. Soc.* **2019**, *141*, 3777.
- [4] S. Balushev, V. Yakutkin, T. Miteva, Y. Avlasevich, S. Chernov, S. Aleshchenkov, G. Nelles, A. Cheprakov, A. Yasuda, K. Mullen, G. Wegner, *Angew. Chem., Int. Ed.* **2007**, *46*, 7693.
- [5] V. Gray, D. Dzebo, M. Abrahamsson, B. Albinsson, K. Moth-Poulsen, *Phys. Chem. Chem. Phys.* **2014**, *16*, 10345.
- [6] B. McKenna, R. C. Evans, *Adv. Mater.* **2017**, *29*, 1606491.
- [7] Y. Y. Cheng, B. Fückel, R. W. MacQueen, T. Khoury, R. G. C. R. Clady, T. F. Schulze, N. J. Ekins-Daukes, M. J. Crossley, B. Stannowski, K. Lips, T. W. Schmidt, *Energy Environ. Sci.* **2012**, *5*, 6953.
- [8] L. Nienhaus, M. Wu, V. Bulović, M. A. Baldo, M. G. Bawendi, *Dalton Trans.* **2018**, *47*, 8509.
- [9] R. S. Khnayzer, J. Blumhoff, J. A. Harrington, A. Haefele, F. Deng, F. N. Castellano, *Chem. Commun.* **2012**, *48*, 209.
- [10] A. Monguzzi, A. Oertel, D. Braga, A. Riedinger, D. K. Kim, P. N. Knüsel, A. Bianchi, M. Mauri, R. Simonutti, D. J. Norris, *ACS Appl. Mater. Interfaces* **2017**, *9*, 40180.
- [11] M. Majek, U. Faltermeier, B. Dick, R. Perez-Ruiz, A. J. von Wangelin, *Chem. - Eur. J.* **2015**, *21*, 15496.
- [12] M. Haring, R. Perez-Ruiz, A. J. von Wangelin, D. D. Diaz, *Chem. Commun.* **2015**, *51*, 16848.
- [13] C. Fan, L. Wei, T. Niu, M. Rao, G. Cheng, J. J. Chruma, W. Wu, C. Yang, *J. Am. Chem. Soc.* **2019**, *141*, 15070.
- [14] Z. Wang, J. Zhao, M. Di Donato, G. Mazzone, *Chem. Commun.* **2019**, *55*, 1510.
- [15] T. W. Schmidt, F. N. Castellano, *J. Phys. Chem. Lett.* **2014**, *5*, 4062.
- [16] V. Gray, A. Dreos, P. Erhart, B. Albinsson, K. Moth-Poulsen, M. Abrahamsson, *Phys. Chem. Chem. Phys.* **2017**, *19*, 10931.
- [17] L. Li, Y. Zeng, J. Chen, T. Yu, R. Hu, G. Yang, Y. Li, *J. Phys. Chem. Lett.* **2019**, *10*, 6239.
- [18] Y. Liu, K. Chen, S. Yang, D. Zheng, G. Ren, Y. Yang, J. Zhao, D. Wei, K. Han, *J. Phys. Chem. Lett.* **2019**, *10*, 4368.
- [19] Y. Wei, M. Zhou, Q. Zhou, X. Zhou, S. Liu, S. Zhang, B. Zhang, *Phys. Chem. Chem. Phys.* **2017**, *19*, 22049.
- [20] Y. Wei, M. Zheng, Q. Zhou, X. Zhou, S. Liu, *Org. Biomol. Chem.* **2018**, *16*, 5598.
- [21] M. Nakashima, K. Iizuka, M. Karasawa, K. Ishii, Y. Kubo, *J. Mater. Chem. C* **2018**, *6*, 6208.
- [22] L. Huang, Y. Zhao, H. Zhang, K. Huang, J. Yang, G. Han, *Angew. Chem., Int. Ed.* **2017**, *56*, 14400.
- [23] Z. Huang, Z. Xu, M. Mahboub, Z. Liang, P. Jaimes, P. Xia, K. R. Graham, M. L. Tang, T. Lian, *J. Am. Chem. Soc.* **2019**, *141*, 9769.
- [24] S. He, X. Luo, X. Liu, Y. Li, K. Wu, *J. Phys. Chem. Lett.* **2019**, *10*, 5036.
- [25] W. Chen, F. Song, S. Tang, G. Hong, Y. Wu, X. Peng, *Chem. Commun.* **2019**, *55*, 4375.
- [26] J. Han, Y. Jiang, A. Obolda, P. Duan, F. Li, M. Liu, *J. Phys. Chem. Lett.* **2017**, *8*, 5865.
- [27] T. C. Wu, D. N. Congreve, M. A. Baldo, *Appl. Phys. Lett.* **2015**, *107*, 031103.
- [28] S. Amemori, Y. Sasaki, N. Yanai, N. Kimizuka, *J. Am. Chem. Soc.* **2016**, *138*, 8702.
- [29] Y. Sasaki, S. Amemori, H. Kouno, N. Yanai, N. Kimizuka, *J. Mater. Chem. C* **2017**, *5*, 5063.
- [30] D. Liu, Y. Zhao, Z. Wang, K. Xu, J. Zhao, *Dalton Trans.* **2018**, *47*, 8619.
- [31] Y. Wei, M. Zheng, L. Chen, X. Zhou, S. Liu, *Dalton Trans.* **2019**, *48*, 11763.
- [32] N. Kimizuka, Y. Sasaki, M. Oshikawa, P. Bharmoria, H. Kouno, A. Hayashi-Takagi, M. Sato, I. Ajioka, N. Yanai, *Angew. Chem., Int. Ed.* **2019**, *58*, 17827.
- [33] V. Gray, D. Dzebo, A. Lundin, J. Alborzpour, M. Abrahamsson, B. Albinsson, K. Moth-Poulsen, *J. Mater. Chem. C* **2015**, *3*, 11111.
- [34] P. Yang, W. Wu, J. Zhao, D. Huang, X. Yi, *J. Mater. Chem.* **2012**, *22*, 20273.
- [35] A. Monguzzi, J. Mezyk, F. Scotognella, R. Tubino, F. Meinardi, *Phys. Rev. B* **2008**, *78*, 195112.
- [36] A. Haefele, J. Blumhoff, R. S. Khnayzer, F. N. Castellano, *J. Phys. Chem. Lett.* **2012**, *3*, 299.
- [37] M. J. Frisch, G. W. Trucks, H. B. Schlegel, G. E. Scuseria, M. A. Robb, J. R. Cheeseman, G. Scalmani, V. Barone, B. Mennucci, G. A. Petersson, H. Nakatsuji, M. Caricato, X. Li, H. P. Hratchian, A. F. Izmaylov, J. Bloino, G. Zheng, J. L. Sonnenberg, M. Hada, M. Ehara, K. Toyota, R. Fukuda, J. Hasegawa, M. Ishida, T. Nakajima, Y. Honda, O. Kitao, H. Nakai, T. Vreven, J. A. Montgomery Jr., et al., *Gaussian 09*, Revision E.01, Gaussian Inc., Wallingford, CT **2009**.